Theoret. Chim. Acta (Berl.) 41, 37-49 (1976)

Theory of Isomer Shift in Hemin*

Jane C. Chang, Yong M. Kim, Tara P. Das

Department of Physics, State University of New York at Albany

Kenneth J. Duff

Department of Physics, University of Wollongong at New South Wales

Received September 10, 1974/April 28, 1975

Using the self-consistent charge extended Hückel procedure, the charge density difference $\Delta\rho$ at Fe^{57} nucleus, between hemin and Fe^{+3} ion is calculated. This is combined with the recent value of the calibration constant, $-0.23\pm0.02a_0^3$ mm/sec to obtain an isomer shift of -0.374 mm/sec between hemin and Fe^{+3} in good agreement with the value -0.392 mm/sec derived from experimental data and the calculated value of the isomer shift of Fe^{+3} with respect to K_3FeF_6 from first principle covalency investigations in the latter compound. $\Delta\rho$ is composed of contributions from core and valence electrons of the same order of magnitude, with the latter being more than one-half of the former. The core contribution is composed of a number of terms of comparable magnitude and differing signs, whose significance is discussed.

Key word: Hemin, isomer shift in ~

1. Introduction

The electronic properties of hemin have been recently subjected to rather extensive theoretical analysis [1–6], using the extended Hückel procedure [7]. This procedure has been successful in earlier investigations in explaining both optical properties [5] as well as a number of hyperfine and magnetic properties [1–4]. For some of the hyperfine properties, there are still some differences with experiment to be explained [2, 4, 6]. The present work is concerned with a theoretical analysis of the various contributions to the isomer shift in the Mössbauer effect of Fe^{57m} in hemin, using Fe^{+3} ion for our reference.

The paper is divided into three sections. The second section will deal briefly with a resumé of the self-consistent charge extended Hückel procedure and the results for the wavefunctions and charge distributions in hemin. The third section will deal with the various contributions to the isomer shift, in particular, the contributions from the valence and core electrons to the charge density at the iron nucleus which is related to the isomer shift. The fourth section will be concerned with a discussion of the results we obtain for the isomer shift, the relative importance

* Supported by grant HL 15196-02 from the Heart and Lung Institute of National Institute of Health.

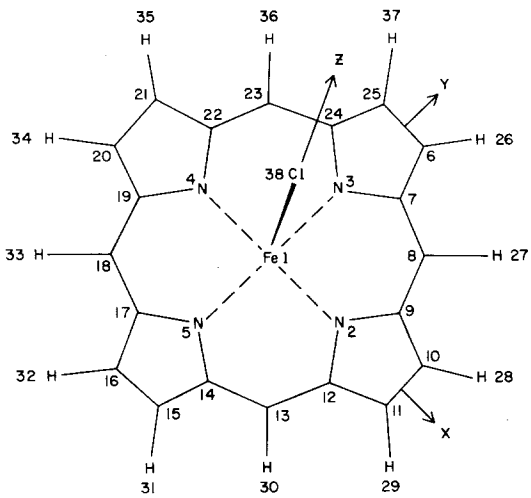

Fig. 1. Molecular structure of iron porphyrin chloride – the model of hemin used here

of valence and core contributions, comparison with experimental data and conclusions that can be drawn regarding the nature of the isomer shift to be expected theoretically in other related compounds.

2. Wave-Functions

The self-consistent charge extended Hückel method that has been used to obtain the molecular wavefunctions of hemin has been described in detail elsewhere [3, 5, 7]. However, we want to discuss some of the parameters, for both the sake of completeness and also because we will require some of them in the calculation of the isomer shift. The coordinates of atoms in the iron-porphyrin system (Fig. 1) used here as representative of hemin are exactly the same as in our previous work [1–4] and those used by Zerner, Gouterman and Kobayashi [5]. Because these are of great interest in the present calculation, we have listed in Table 1 the coordinates of four nitrogens, eight carbons of porphyrin rings that are nearest to the iron, and the chlorine atom attached to heme, with the atoms being numbered as in Fig. 1. We have taken the position of the iron atom as being 0.455 Å above the porphyrin plane in keeping with earlier work [3], although the X-ray data of Koenig [8] seems to indicate that it is a little different, namely 0.475 Å.

In the wave-function calculation, one determines the molecular orbitals (MO) in the form:

$$\psi_\mu = \sum_i C_{\mu i}\chi_i \tag{1}$$

where $C_{\mu i}$ is the coefficient for the i^{th} atomic orbital (AO) χ_i in the μ^{th} MO ψ_μ. The $C_{\mu i}$'s are determined by solving the appropriate secular equation. In formulating the secular equation, one needs the matrix elements h_{ii} and h_{jj} of the Hamiltonian and S_{ij}, the elements of the overlap matrix, which are taken as the same

Table 1. Geometry of atoms in iron(III) porphyrin chloride (model used for hemin)

Atoms[a]	X(Å)	Y(Å)	Z(Å)
Fe(1)	0	0	0.455
N(2)	2.054	0	0
N(3)	0	2.054	0
N(4)	−2.054	0	0
N(5)	0	−2.054	0
C(7)	1.098	2.839	0
C(9)	2.839	1.098	0
C(12)	2.839	−1.098	0
C(14)	1.098	−2.839	0
C(17)	−1.098	−2.839	0
C(19)	−2.839	−1.098	0
C(22)	−2.839	1.098	0
C(24)	−1.098	2.839	0
Cl(38)	0	0	2.67

[a] The numbering of atoms and the designation of X and Y axes are shown in Fig. 1.

as those utilized in earlier work [3][1]. The matrix elements h_{ii} were related to the charges on the atom, which in turn are obtained from $C_{\mu i}$ through the Mulliken approximation [9]. The convergence is characterized by the closeness of the input and output charges. In analyzing this convergence, we utilized the following equation for the charge q_l^λ on the l^{th} atom for the λ^{th} iteration, namely

$$q^{\lambda}_{l,\,input} = \frac{w q^{\lambda-1}_{l,\,input} + q^{\lambda-1}_{l,\,output}}{w+1} \tag{2}$$

the parameter w being chosen judiciously to speed convergence, a convenient value to use at the start of the iterations being in the range 10 to 20. The convergence criterion used was

$$\left|q^{\lambda}_{l,\,input} - q^{\lambda}_{l,\,output}\right| \leqslant 0.05 \tag{3}$$

Since the final charges and the nature of the convergence of the calculation have not been discussed in our earlier publications on properties of hemin and since it may be of some interest to other workers in the field, we have presented in Fig. 2, the charges of typical atoms at various stages of iteration. The charges on the rest of the atoms can be related to these by symmetry. The final charges on the atoms, corresponding to the molecular orbital wave-function, are listed in Table 2 and are fairly close to those of Zerner, Gouterman and Kobayashi [5]. From Fig. 2 it appears that in the intermediate iterative stages, the major oscillation does occur around iron. This is not unexpected, since the iron atom is the main source of charge transfer, the charge being +3 on the extreme crystal field model

[1] The Slater orbitals used in the calculation of overlap matrix elements in the secular equation have been chosen to reproduce the same overlap integrals as with the actual SCF atomic orbitals. However, the Slater orbitals do not have the correct behavior near the nucleus which is important for hyperfine properties.

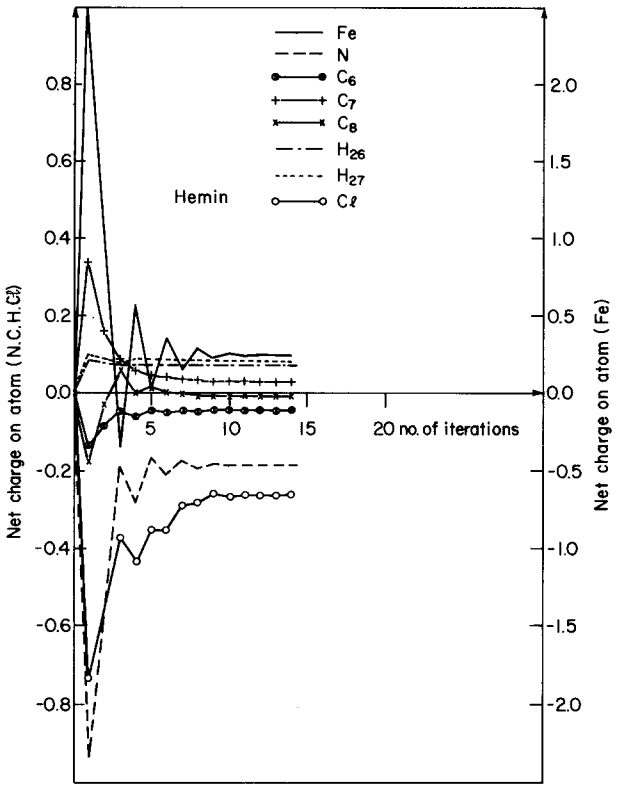

Fig. 2. Distribution of net charges among atoms for various iterations

with no interactions with the rest of the ring. As we notice from the final charges on the iron atom, and in general the charges on the rest of the atoms in the molecule, they are actually rather close to neutrality. The final electronic configuration of iron that is obtained in the Mulliken approximation from our calculations is: $(1s)^2(2s)^2(2p)^6(3s)^2(3p)^6(3d)^{6.74}(4s)^{0.41}(4p)^{0.60}$. This configuration is fairly close to that of neutral iron atom and even closer to the $3d^74s$ configuration of iron in the metal [10] for which the wave functions are also available. For calculation of properties involving the regions near the nuclei it is important to use the actual atomic orbitals in Eq.(1) for the MO instead of the Slater-like orbitals that are used [3] in obtaining the overlap matrix S in the secular equation.

3. Isomer Shift

The isomer shift for the same nucleus in two chemical environments is given by the relation: [11]

$$\varepsilon_1 - \varepsilon_2 = \alpha[\rho_1(0) - \rho_2(0)] \tag{4}$$

ε_1 and ε_2 being Mössbauer frequencies for the two sources. The isomer shift proportionality constant parameter α depends on the properties of the nucleus,

Table 2. Final charge distributions[a] of hemin obtained from the self-consistent charge Hückel procedure

Atom	Charge	Atom	Charge
1	0.2507	20	−0.04305
2	−0.1759	21	−0.04305
3	−0.1759	22	0.03282
4	−0.1759	23	−0.01626
5	−0.1594	24	0.03282
6	−0.04305	25	−0.04305
7	0.03282	26	0.06163
8	−0.01626	27	0.08774
9	0.03282	28	0.06163
10	−0.04305	29	0.06163
11	−0.04305	30	0.08775
12	0.03282	31	0.06163
13	−0.01626	32	0.06163
14	0.03282	33	0.08775
15	−0.04305	34	0.06163
16	−0.04305	35	0.06163
17	0.03282	36	0.08774
18	−0.01626	37	0.06163
19	0.03282	38	−0.2439

[a] The numbering of the atoms is as in Fig. 1.

namely, its nuclear charge, atomic mass number, the fractional change in nuclear charge radius during the γ-ray transition, and the γ-ray energy. $\rho_1(0)$ and $\rho_2(0)$ are the electron densities at the nuclei for the two systems. Unfortunately, one cannot get a value of α accurately from the theory of nuclear structure. Instead, one has to obtain α by using the experimental $\varepsilon_1 - \varepsilon_2$ in a pair of systems and the difference in the two $\rho(0)$ on the right hand side of Eq.(4), which has to be calculated accurately for the two systems. The determination of α has been carried out by a number of investigators in the past few years. These have been reviewed in a recent article [12] where a first-principle covalency calculation for K_3FeF_6 is done, using a model of a ferric ion surrounded by six F^- ions in a cubic arrangement. This charge density has been compared with that in a ferrous compound to evaluate α. The value α obtained was $-0.23 \pm 0.02\ a_0^3$ mm s^{-1} and the relation between this value of α and earlier ones was discussed [12, 13][2]. Further, recently, an evaluation of many-body effects on the charge densities in Eq.(4) has been

[2] The value of α is assumed (Ref. [12]) to include the relativistic correction so that it has to be used in conjunction with non-relativistic electronic densities at the iron nucleus. This process of incorporating the relativistic effect on α is strictly justified if the relativistic correction is nearly the same for all the s-orbitals of the iron atom in the compounds involved. There have been arguments for both sides of this question in the literature [13]. Our present study of the isomer shift in hemin is not aimed at obtaining very precise quantitative agreement with experiment but rather at an examination of its origin from a semi-quantitative point of view with the purpose of assessing if one could use the presently used procedures to explain the small variations between a number of heme compounds. We shall therefore not be concerned with the question of the proper incorporation of relativistic effects, and shall utilize the non-relativistic result for the density at the nucleus and the value of $\alpha = -0.23 a_0^3$ mm sec^{-1} in our isomer shift analysis.

carried out [14] through the linked cluster many-body perturbation theory. These effects have been found to be rather small in their influence on α derived from isomer shift between Fe^{+3} and Fe^{+2} compounds. We shall therefore use $\alpha = -0.23\ a_0^3$ mm s^{-1} in obtaining the isomer shift in hemin.

Next, we have to consider the values of $\rho_1(0)$ and $\rho_2(0)$ in Eq.(4) with 1 referring to hemin and 2 to a reference system. In our work here, we shall make use of Fe^{+3} ion as a reference system. There is no experimental value available for the isomer shift of hemin with respect to Fe^{+3} ion. To compare with experiment, we shall therefore follow two steps. First we shall convert the measured [15] isomer shift of hemin with respect to cobalt in platinum to K_3FeF_6 as reference system using experimental data [16, 17] on the isomer shift of K_3FeF_6 and some other systems. The second step will involve use of the calculated isomer shift of K_3FeF_6 with respect to Fe^{+3} ion from recent first-principle covalency investigations [12] on this system.

The charge density $\rho(0)$ is given by the expectation value of the charge density operator $\rho_{op}(0)$

$$\rho_{op}(0) = \sum_i \delta(\vec{r}_i) \tag{5}$$

over the determinental wavefunction ψ involving both the core and valence orbitals of hemin. The summation over i runs over all the electrons in the system which consist of both paired and unpaired electrons as well as the core electrons of the atoms, particularly those of the iron atom. The core electrons of neighboring atoms are not expected to contribute too much to the density at the iron nucleus so they can be dropped. But we must include contributions from both the valence and the core electrons of iron. If all the core electrons and valence electron orbitals were orthogonal to each other then ρ will be given by

$$\rho(0) = \langle \psi | \rho_{op}(0) | \psi \rangle = \sum_v |\psi_v(0)|^2 n_v \tag{6}$$

the ψ_v being one-electron wave-functions of the system and $n_v = 2$, 1 or 0 represents the number of electrons in the orbital v. The summation over v extends over the core orbitals of iron and the occupied valence orbitals. However, the summation in Eq.(6) is only correct as far as valence orbitals are concerned, since they are mutually orthogonal. The core orbitals, however, are not orthogonal to the valence orbitals and one thus has to take into account the overlap of the core and valence orbitals. It has been demonstrated in several calculations [18] involving non-orthogonal core orbitals that one can still use the summation in Eq.(6) provided one makes the core orbitals orthogonal to the valence orbitals by the Schmidt or some other orthogonalization procedure. We shall adopt the Schmidt procedure here and therefore replace $1s$, $2s$ and $3s$ core wave-functions by functions that are orthogonal to the valence wave-functions and to each other. The latter requirement is pertinent, because if we merely orthogonalized the core orbitals individually to the valence orbitals, these orthogonalized core-orbitals would not be orthogonal to each other. The mutually orthogonalized core wave-functions are given by:

$$\psi_{1s}^{\text{ortho}}=\frac{\psi_{1s}-\sum_{\mu} S_{1s,\mu}\psi_{\mu}}{\sqrt{1-\sum_{\mu} S_{1s,\mu}^2}}$$

$$\psi_{2s}^{\text{ortho}}=\frac{\psi'_{2s}-\langle\psi'_{2s}|\psi_{1s}^{\text{ortho}}\rangle\psi_{1s}^{\text{ortho}}}{\sqrt{1-|\langle\psi'_{2s}|\psi_{1s}^{\text{ortho}}\rangle|^2}} \tag{7}$$

$$\psi_{3s}^{\text{ortho}}=\frac{\psi'_{3s}-\langle\psi'_{3s}|\psi_{2s}^{\text{ortho}}\rangle\psi_{2s}^{\text{ortho}}-\langle\psi'_{3s}|\psi_{1s}^{\text{ortho}}\rangle\psi_{1s}^{\text{ortho}}}{\sqrt{1-|\langle\psi'_{3s}|\psi_{2s}^{\text{ortho}}\rangle|^2-|\langle\psi'_{3s}|\psi_{1s}^{\text{ortho}}\rangle|^2}}$$

where

$$\psi'_{2s}=\frac{\psi_{2s}-\sum_{\mu} S_{2s,\mu}\psi_{\mu}}{\sqrt{1-\sum_{\mu} S_{2s,\mu}^2}}$$

$$\psi'_{3s}=\frac{\psi_{3s}-\sum_{\mu} S_{3s,\mu}\psi_{\mu}}{\sqrt{1-\sum_{\mu} S_{3s,\mu}^2}} \tag{8}$$

In Eqs.(7) and (8)

$$S_{ns,\mu}=\langle\psi_{ns}|\psi_{\mu}\rangle$$

is the overlap integral between the core ψ_{ns} orbital and the occupied valence orbitals ψ_{μ}. The summation is over all valence orbitals occupied by the electrons of the same spin. From Eqs.(8) it follows that

$$\langle\psi'_{2s}|\psi_{1s}^{\text{ortho}}\rangle=\frac{-\sum S_{1s,\mu}S_{2s,\mu}}{\sqrt{(1-\sum_{\mu} S_{1s,\mu}^2)(1-\sum_{\mu} S_{2s,\mu}^2)}} \tag{9}$$

with corresponding expressions for $\langle\psi'_{3s}|\psi_{1s}^{\text{ortho}}\rangle$ and $\langle\psi'_{3s}|\psi_{2s}^{\text{ortho}}\rangle$.

In terms of the valence orbital and orthogonalized core orbital wave-functions, the charge density at the iron-site can then be written as

$$\rho(0)=\sum_{\mu=1}^{M} 2|\psi_{\mu}(0)|^2+\sum_{\mu=M+1}^{N}|\psi_{\mu}(0)|^2+\sum_{n=1}^{3}[|\psi_{ns\uparrow}^{\text{ortho}}(0)|^2+|\psi_{ns\downarrow}^{\text{ortho}}(0)|^2] \tag{10}$$

where $\mu=1$ to M represents the number of orbitals that are doubly occupied, $\mu=M+1$ to N represents singly occupied orbitals and the last term corresponds to a sum over the orthogonalized cores, the subscripts $\uparrow$ and $\downarrow$ referring to spins parallel and antiparallel to the unpaired valence electrons. The valence orbitals $\psi_{\mu}(\mu=1$ to $N)$'s, as defined in Eq.(1) of Sect. 2, are taken with the molecular orbital coefficients $C_{\mu i}$ determined from the extended Hückel calculation but with the atomic orbitals χ_i at the iron site replaced by Hartree-Fock orbitals. One then gets

$$\rho_{\text{valence}}=\sum_{\mu=1}^{M} 2|\psi_{\mu}(0)|^2+\sum_{\mu=M+1}^{N}|\psi_{\mu}(0)|^2=\rho_{\text{val}}^{(2)}+\rho_{\text{val}}^{(1)} \tag{11}$$

where

$$|\psi_\mu(0)|^2 = |\sum_i C_{\mu i}\chi_i(0)|^2$$

In Table 3, we have separated the contributions to the density from the valence orbitals of hemin as composed of those from doubly occupied orbitals $\rho_{\text{val}}^{(2)}$ and from singly occupied orbitals $\rho_{\text{val}}^{(1)}$. The major contributions arise out of the doubly occupied orbitals 1, 8, 12, 14, 46, 47 which all involve significant amounts of iron 4*s* character. Among the unpaired occupied orbitals only one makes a finite contribution, namely orbital 65 which is primarily of d_{z^2} character but hybridized to 4*s*. The net contribution from the valence orbitals is given by

$$\rho_{\text{val}} = 0.6716 a_0^{-3} \tag{12}$$

For the core contributions one has to obtain the $|\psi_{ns}^{\text{ortho}}(0)|^2$ using the orthogonalized functions $\psi_{ns}^{\text{ortho}}(r)$.

The core-contribution to the density $\Delta\rho_{\text{core}}$, are obtained by comparing the density due to core states on hemin with that in ferric ion. There are two kinds of contributions that can occur. One is the difference between the densities due to non-orthogonalized cores and the orthogonalized cores in hemin. This represents the influence of Pauli principle on the core orbitals. The second difference is the result of the different potentials seen by the cores in Fe^{+3} ion and in hemin, the contribution to this potential due to the valence electrons being influenced by molecular orbital formation. This difference in densities is essentially given by the difference between the densities due to unorthogonalized hemin and ferric ion core orbitals. This second difference would not occur in a crystal field model involving a Fe^{+3} ion located at the iron site in hemin. These two core contributions thus represent respectively the influence of Pauli and potential distortions. The unorthogonalized core functions in hemin correspond to the neutral iron atom.

Thus the two types of contribution to the charge density difference between hemin core orbitals and Fe^{+3} ion core orbitals can be written as

$$\Delta\rho_{\text{Pauli}} = \sum_{n=1}^{3} |\psi_{ns}(0)|^2 \sum_\mu S_{ns,\mu}^2 - 2\sum_{n=1}^{3} \psi_{ns}(0) \sum_\mu S_{ns,\mu}\psi_\mu(0) + 2\sum_{n>m} \psi_{ns}(0)\psi_{ms}(0) \sum_\mu S_{ns,\mu}S_{ms,\mu} \tag{13}$$

Table 3. Direct valence contribution[a] ρ_{val} to the charge density at iron in hemin

$\rho_{\text{val}}^{(1)}$	$0.0078 a_0^{-3}$
$\rho_{\text{val}}^{(2)}$	$0.6638 a_0^{-3}$
ρ_{val}	$0.6716 a_0^{-3}$

[a] $\rho_{\text{val}}^{(1)}(0)$, $\rho_{\text{val}}^{(2)}(0)$ and $\rho_{\text{val}}(0)$ are the direct contributions of singly occupied valence orbitals, of doubly occupied valence orbitals and of all valence orbitals, respectively.

which follows from Eqs.(7) and

$$\Delta\rho_{\text{pot}}=\sum_{n}\left[\left|\Psi_{ns}^{\text{neutral}}(0)\right|^2-\left|\Psi_{ns}^{Fe^{+3}}(0)\right|^2\right] \tag{14}$$

In Eq.(13) only terms of second-order in overlap between the core and valence orbitals are included, terms like the second one in Eq.(13), are considered as second order since they involve one order in the amplitude of the valence wave-function at the iron nucleus in addition to one order in overlap. The total core density difference between hemin and Fe^{+3} is given by:

$$\Delta\rho_{\text{core}}=\Delta\rho_{\text{Pauli}}+\Delta\rho_{\text{pot}} \tag{15}$$

In $\Delta\rho_{\text{Pauli}}$, we have three terms in Eq.(13), the three being referred to respectively as renormalization, valence-core cross and reorthogonalization terms. One need not have made a separation into these terms and could have just used the sum of the differences between $\left|\Psi_{ns}^{\text{ortho}}(0)\right|^2$ and $\left|\Psi_{ns}^{\text{neutral}}(0)\right|^2$. The difference between the result obtained in this way and according to Eq.(13) involves terms that are higher than second order in overlap and give very little contribution to the isomer shift. From the interest of computational accuracy, it is perhaps better to use Eq.(13) rather than the difference in large numbers that one would get from $\left|\Psi_{ns}^{\text{ortho}}(0)\right|^2$ and $\left|\Psi_{ns}^{\text{neutral}}(0)\right|^2$. In addition, the separation of $\Delta\rho_{\text{Pauli}}$ into three parts according to their origins does provide additional physical insight.

In Table 4, we have tabulated the pertinent quantities such as overlap factors and wave-function amplitudes for the neutral atom[3] and Fe^{+3} ion that go into the evaluation of $\Delta\rho_{\text{Pauli}}$ and $\Delta\rho_{\text{pot}}$. In Table 5, the various contributions to $\Delta\rho_{\text{Pauli}}$ and also $\Delta\rho_{\text{pot}}$ are tabulated for the various core-states. For the two different spin-states there are slight differences because there are more valence orbitals with one spin-state to which the corresponding core orbitals of the same spin-state have to be orthogonalized than for the other spin-state. An important feature of the results in Table 5 is that all the contributions to $\Delta\rho_{\text{Pauli}}(0)$ and $\Delta\rho_{\text{pot}}(0)$ are comparable and dropping any of these would not be meaningful. In particular, the potential terms, which would be neglected if one used a crystal field type model of a Fe^{+3} ion unbonded [20] to the rest of the orbitals, make important cancellations with $\Delta\rho_{\text{Pauli}}$ for the $2s$ and $3s$ states and add in the case of the $1s$ state. It should be remarked however that practically all of the contributions in the

[3] In the calculation of the results in Table 4, Mann's numerically tabulated functions have been used for Fe^{+3} core amplitudes. For the evaluation of overlaps in the calculation of the Pauli contribution, we have utilized Hartree-Fock wave-functions in analytic form obtained for the $3d^74s$ configuration. However, in calculating the amplitudes at the nucleus for the core wave-functions, we have used Mann's numerically tabulated core-electron wave-functions for the $3d^64s^2$ configuration (J. B. Mann, Atomic Structure Calculation, II Hartree-Fock Wavefunctions and Radial Expectation Values: Hydrogen to Lawrencium, Report LA3691, Los Alamos Scientific Laboratory of University of California, Los Alamos, New Mexico (1969)). The reasons for the latter choice are first that it is difficult to get accurate amplitudes at the nucleus from analytic wave-functions. Secondly, as shown by Duff [12], in taking differences between densities at the nucleus for two configurations, it is necessary to use wave-functions calculated by the same procedure and since Mann's numerical wave-functions were used for Fe^{+3} ion, it is desirable to use Mann's wave-functions also for the neutral atom as well. Finally, Mann's numerical core wave-functions were found overall, particularly in the inner regions of the atom, to be quite close to those for the $3d^74s$ configuration.

Table 4. List of pertinent quantities important for core-contribution to isomer shift

Core state	Overlap factor for renormalization term		Overlap factor for valence-core cross term $-\sum_i S_{ns,i}\phi_i$		Overlap factor for reorthogonalization term $\sum_i S_{ns,i}S_{ms,i}$		Neutral atom core state wave-function amplitude $\lvert\phi^0_{ns}(0)\rvert$	Fe^{+3} ion wave-function amplitude $\lvert\phi^0_{ns}(0)\rvert$
	up	down	up	down	up	down		
1*s*	0.00000861	0.00000861	0.0013993	0.0013975	0	0	73.4010	73.4000
2*s*	0.0004637	0.0004636	−0.0102698	−0.010255	-6.3177×10^{-5}	-6.3173×10^{-5}	22.2609	22.2591
3*s*	0.015313	0.015308	0.059302	0.059098	-2.6588×10^{-3} 3.6207×10^{-4}	-2.6585×10^{-3} 3.6202×10^{-4}	8.2547	8.3177

Table 5. List of core contributions to hemin-Fe^{+3} charge density

Core state		Renormalization term $\phi^2_{ns}(0)\sum S^2_{ni}$	Valence-core cross term $-2\sum S_{ns,i}\phi_i\phi_{ns}(0)$	Reorthogonalization term $2\sum_i S_{ns,i}S_{ms,i}\phi_{ms}(0)\phi_{ns}(0)$	Net overlap term $\Delta\rho_{\text{Pauli}}$	Potential term $\Delta\rho_{\text{pot}}$	Net hemin Fe^{+3} core density difference $\Delta\rho_{\text{core}}$
1*s*	up	0.04639	0.2054	0	0.2518	0.2792	0.7826
	down	0.04639	0.2052	0	0.2515		
2s	up	0.2298	−0.4572	−0.2065	−0.4339	0.1630	−0.7042
	down	0.2297	−0.4566	−0.2064	−0.4333		
3*s*	up	1.0436	0.9790	−0.9772 0.4388	1.4841	−2.0896	0.8749
	down	1.0431	0.9757	−0.9770 0.4387	1.4804		
Total		2.6388	1.4514	−1.4896	2.6007	−1.6474	0.9533

reorthogonalization terms comes from terms involving the 4*s* component of the molecular orbitals. Terms involving products of iron atom orbital amplitudes and neighboring atom orbital amplitudes which can be referred to as [21] non-local terms and the distant terms, involving the products of neighboring atom orbital amplitudes make rather small contributions. Thus almost the entire contribution to $\Delta\rho(0)$ is local in origin.

The above analysis of our results has shown that the valence electrons have importance for the isomer shift due to a number of reasons. First, one has of course to include their contributions to the density directly because this effect is sizeable, as seen from Eq.(12), namely about more than one half of the core contribution in the present case. This point has been demonstrated also by recent covalency calculations in ionic crystals [12]. Secondly, the valence orbitals also play a significant indirect role through their influence on the core contribution in two ways, the potential and Pauli overlap effects, both of which we have considered above.

The net theoretical result for $|\rho_{\text{hemin}}(0)| - |\rho_{Fe^{+3}}(0)|$ is given by combining the valence and core contributions, namely,

$$\rho_{\text{hemin}} - \rho_{Fe^{+3}} = 1.625 a_0^{-3} \tag{16}$$

Using this density difference and the values [12] of $\alpha = -0.23 a_0^3$ mm sec^{-1}, we get

$$\varepsilon_{\text{hemin}} - \varepsilon_{Fe^{+3}} = -0.374 \text{ mm/sec} \tag{17}$$

4. Discussion

There is no direct measurement of isomer shift between hemin and a free Fe^{+3} ion. We have therefore to derive it by combining the isomer shifts in a number of related systems. Thus, there exists a measurement [15] of the isomer shift in hemin with respect to a cobalt source in platinum. This result can be combined with the measurement of isomer shift in nitroprusside [17] with respect to cobalt source in platinum for which data is available. The two above data, when combined, give the isomer shift of hemin with respect to nitroprusside. These data can in turn be combined with available data for isomer shift [17] of nitroprusside with respect to stainless steel. One next uses the available isomer shift data [16] for K_3FeF_6 with respect to FeF_2 and of the latter [17] with respect to stainless steel to get the isomer shift for hemin with respect to K_3FeF_6. Finally a combination of these results is made with the calculated isomer shift of K_3FeF_6 with respect to Fe^{+3} to get the isomer shift of hemin with respect to Fe^{+3} to compare with our theoretical result in Eq.(17). The process of combination is shown in the Eqs.(18):

$$\begin{aligned}
&\varepsilon_{\text{hemin}} - \varepsilon_{\text{Fe in Pt.}} = 0.09 \text{ mm/sec} \\
&\varepsilon_{\text{Fe in Pt.}} - \varepsilon_{\text{nitroprusside}} = 0.607 \text{ mm/sec} \\
&\varepsilon_{\text{nitroprusside}} - \varepsilon_{\text{stainless steel}} = -0.175 \text{ mm/sec} \\
&\varepsilon_{\text{stainless steel}} - \varepsilon_{FeF_2} = -1.4 \text{ mm/sec} \\
&\varepsilon_{FeF_2} - \varepsilon_{K_3FeF_6} = 0.93 \text{ mm/sec} \\
&\varepsilon_{K_3FeF_6} - \varepsilon_{Fe^{+3}} = -0.437 \text{ mm/sec}
\end{aligned} \tag{18}$$

leads to

$$\varepsilon_{\text{hemin}} - \varepsilon_{Fe^{+3}} = -0.385 \text{ mm/sec} \tag{19}$$

A second way to derive the isomer shift of hemin with respect to Fe^{+3} is the following. One can use available experimental data [22] for hemin with respect to iron in copper, combine this with the isomer shift [17] of iron in copper with respect to nitroprusside to get the isomer shift of hemin with respect to nitroprusside. From this information, one gets to Fe^{+3} through stainless steel, FeF_2 and K_3FeF_6 in the same way as above. This alternate avenue is indicated in Eqs.(20) and (21).

$$\begin{aligned} \varepsilon_{\text{hemin}} - \varepsilon_{\text{Fe in Cu}} &= 0.2 \text{ mm/sec} \\ \varepsilon_{\text{Fe in Cu}} - \varepsilon_{\text{nitroprusside}} &= 0.483 \text{ mm/sec} \\ \varepsilon_{\text{nitroprusside}} - \varepsilon_{Fe^{+3}} &= -1.082 \text{ mm/sec} \end{aligned} \tag{20}$$

leading to

$$\varepsilon_{\text{hemin}} - \varepsilon_{Fe^{+3}} = -0.399 \text{ mm/sec} \tag{21}$$

The two answers in Eqs.(20) and (21) derived from combination of different experimental data thus agree with each other within a factor of better than 5%. It is reasonable therefore to take the mean of these two results, i.e. -0.392 mm/sec as the value to compare with our result in Eq.(17). The experimental result carries a probable uncertainty of about 0.05 mm/sec due to the fact that the rest of the experimental data used in Eqs.(18) and (20), besides that for hemin, are for room temperature while the latter is at liquid helium temperature. There is good agreement between the experimental result and theoretical value in Eq.(17). The agreement is better than we had expected because of the approximations involved in the extended Hückel procedure. It does show that the extended Hückel approach provides a reasonable description of the total charge density at the nuclei which is composed of valence and core contributions of comparable order of magnitude. As far as the valence contribution is concerned, the fact that we obtain a reasonable charge description with the extended Hückel approach is not surprising, because the extended Hückel approach we have used here involves self-consistency in the charge distribution. The fact that the core contribution appears to be also satisfactory indicates that it is important to incorporate the two effects that we have considered, namely, the Pauli effect and the potential effect. If we had neglected the latter, namely, the difference between the free ferric ion density and the core density in hemin (excluding overlap effects) which corresponds closely to the neutral atom, we would have obtained rather poor agreement with experiment. For a theoretical understanding of the isomer shifts in more complicated systems [23] involving ligands joining hemin to proteins as in methemoglobin or in hemoglobin fluoride one must therefore take into account all of the contributions considered here, namely, the valence and core Pauli and potential terms if one is to aim at a satisfactory agreement similar to that obtained here for hemin. Since all these terms are sizeable and involve positive and negative signs, their variations could well combine to explain the substantial observed isomer shifts between hemin and methemoglobin and hemoglobin fluoride.

References

1. Han,P.S.; Das,T.P., Rettig,M.F.: J. Chem. Phys. **56**, 3861 (1972)
2. Han,P.S., Rettig,M.F., Ikenberry,D., Das,T.P.: Theoret. Chim. Acta (Berl.) **22**, 261 (1971)
3. Han,P.S., Das,T.P., Rettig,M.F.: Theoret. Chim. Acta (Berl.) **16**, 1 (1970)
4. Rettig,M.F., Han,P.S., Das,T.P.: Theoret. Chim. Acta (Berl.) **12**, 178 (1968); Erratum. Theoret. Chim. Acta (Berl.) **13**, 432 (1969)
5. Zerner,M., Gouterman,M., Kobayashi,H.: Theoret. Chim. Acta (Berl.) **6**, 363 (1966); Zerner,M., Gouterman,M.: Theoret. Chim. Acta (Berl.) **4**, 44 (1966)
6. Chang,J.C., Das,T.P., Ikenberry,D.: Theoret. Chim. Acta (Berl.) **35**, 361 (1974)
7. Hoffman,R.: J. Chem. Phys. **39**, 1397 (1963)
8. Koenig,D.F.: Acta Cryst. **18**, 663 (1965)
9. Mulliken,R.S.: J. Chem. Phys. **23**, 1833 (1955)
10. Duff, K. J., Das,T.P.: Phys. Rev. **B3**, 192; 2294 (1971)
11. Shirley,D.A.: Rev. Mod. Phys. **36**, 339 (1964)
12. Duff,K.J.: Phys. Rev. **B9**, 66 (1974)
13. Micklitz,H., Litterst,F.L.: Phys. Rev. Letters **33**, 480 (1974); Trautwein,A., Harris,F.E., Freeman, A.J., Desclaux,J.P.: Phys. Rev. (in press)
14. Ray,S.N., Lee,T., Das,T.P.: Phys. Rev. **B12**, 58 (1975)
15. Gonser,U., Grant,R.W.: Biophys. J. **5**, 823 (1965)
16. Champion,V.I., Vaughan,R.W., Drickamer,H.G.: J. Chem. Phys. **47**, 2583 (1967)
17. Danon,J., in: Chemical applications of Mössbauer spectroscopy, Chapt. 3, Tables 3.28 and 3.34. Goldanski,V.I. and Herber,R.H., Eds. New York: Academic Press,
18. Gourary,B.S., Adrian,F.J.: Phys. Rev. **105**, 1180 (1957). See also Ikenberry,D., Das,T.P.: Phys. Rev. **B1**, 1219 (1970) and Refs. therein
19. The Hartree-Fock functions used for ferric ion were kindly supplied by Dr. J. B. Mann, Radiation Laboratory of University of California, Los Alamos, New Mexico (1968)
20. Such a model has been used in recent calculations by Sharma,R.R. and Moutsos,P. as reported in Bull. Amer. Phys. Soc. **19**, 1101 (1974). See also Moutsos,P., Adams III,J.G. and Sharma,R.R.: J. Chem. Phys. **60**, 1447 (1974). They consider only the Pauli effect arising from overlap of the Fe^{+3} ions with the atomic orbitals of the nitrogen, chlorine and carbon atoms. K. J. Duff (J. Chem. Phys. **63**, 2259 (1975)) has recently commented on the difficulties in the approach used by the authors.
21. Ikenberry,D., Das,T.P.: Phys. Rev. **184**, 989 (1969)
22. Bearden,A.J., Moss,T.H., Caughey,W.S., Beaudreau,C.A.: Proc. Natl. Acad. Sci. U.S. **53**, 1246 (1965)
23. Lang,G., Marshall,W.: Proc. Phys. Soc. **87**, 3 (1966)

Prof. Dr. T. P. Das
Department of Physics
State University of New York at Albany
1400 Washington Avenue
Albany, N.Y. 12222, USA